This article has been accepted for publication in a future issue of this journal, but has not been fully edited. Content may change prior to final publication. Citation information: DOI 10.1109/TSG.2017.2693121, IEEE Transactions on Smart Grid

Dynamic Price Vector Formation Model Based Automatic Demand Response Strategy for PV-assisted EV Charging Stations

Qifang Chen, *Student Member, IEEE,* Fei Wang, *Member, IEEE*, Bri-Mathias Hodge, *Senior Member, IEEE,* Jianhua Zhang, *Member, IEEE,* Zhigang Li, *Member, IEEE,* Miadreza Shafie-khah, *Member, IEEE* and João P. S. Catalão, *Senior Member, IEEE*

***Abstract*—A Real-Time Price (RTP) based Automatic Demand Response (ADR) strategy for PV-assisted Electric Vehicle (EV) Charging Station (PVCS) without Vehicle to Grid (V2G) is proposed. The charging process is modeled as a Dynamic Linear Program (DLP) instead of the normal day-ahead and real-time regulation strategy, to capture the advantages of both global and real-time optimization. Different from conventional price forecasting algorithms, a Dynamic Price Vector Formation Model (DPVFM) is proposed based on a clustering algorithm to form a RTP vector for a particular day. A Dynamic Feasible Energy Demand Region (DFEDR) model considering grid voltage profiles is designed to calculate the lower and upper bounds. A deduction method is proposed to deal with the unknown information of future intervals, such as the actual stochastic arrival and departure times of EVs, which make the DFEDR model suitable for global optimization. Finally, both the comparative cases articulate the advantages of the developed methods and the validity in reducing electricity costs, mitigating peak charging demand, and improving PV self-consumption of the proposed strategy are verified through simulation scenarios.**

***Index Terms*—Automatic demand response, charging station, electric vehicle, real-time price, PV system.**

This work was supported in part by the National Natural Science Foundation of China (grant No. 51577067), the Natural Science Foundation of Beijing (grant No. 3162033), the Natural Science Foundation of Hebei (grant No. E2015502060), the State Key Laboratory of Alternate Electrical Power System with Renewable Energy Sources (grant No. LAPS16007, LAPS16015), the Major Key Science and Technology Project in Renewable Energy Area of Yunnan Province (No. 2013ZB005), the China Scholarship Council and the Science & Technology Project of Yunnan Power Grid Co., Ltd (No. YNKJQQ00000280). This work was also supported by the U.S. Department of Energy under Contract No. DE-AC36-08-GO28308 with the National Renewable Energy Laboratory. Moreover, J.P.S. Catalão acknowledges the support by FEDER funds through COMPETE 2020 and by Portuguese funds through FCT, under Projects SAICT-PAC/0004/2015 - POCI-01-0145-FEDER-016434, POCI-01-0145-FEDER-006961, UID/EEA/50014/2013, UID/CEC/50021/2013, and UID/EMS/00151/2013, and also funding from the EU 7th Framework Programme FP7/2007-2013 under GA no. 309048. *(Corresponding author: Fei Wang.)*

Q. Chen, F. Wang and J. Zhang are with the State Key Laboratory of Alternate Electrical Power System with Renewable Energy Source (North China Electric Power University), Beijing 102206, Baoding 071003, China. Q. Chen and F. Wang are also with the Department of Electrical and Computer Engineering, University of Illinois at Urbana-Champaign, Urbana, IL 61801, USA (e-mail: wangfei@illinois.edu).

B.-M. Hodge is with the National Renewable Energy Laboratory, Golden, CO 80401 USA (e-mail: bri-mathias.hodge@nrel.gov).

Z. Li is with South China University of Technology, Guangzhou 510006, China (e-mail: lizg16@scut.edu.cn).

M. Shafie-khah is with C-MAST, University of Beira Interior, Covilhã 6201-001, Portugal (e-mail: miadreza@gmail.com)

J. P. S. Catalão is with INESC TEC and the Faculty of Engineering of the University of Porto, Porto 4200-465, Portugal, also with C-MAST, University of Beira Interior, Covilhã 6201-001, Portugal, and also with INESC-ID, Instituto Superior Técnico, University of Lisbon, Lisbon 1049-001, Portugal (e-mail: catalao@ubi.pt).

I. Nomenclature

Abbreviations

ADR	Automatic Demand Response
EV	Electric Vehicle
PV	Photovoltaic
DFEDR	Dynamic Feasible Energy Demand Region
DPVFM	Dynamic Price Vector Formation Model
SOC	State of Charge.
DLP	Dynamic Linear Programming

Variables

Δt	The length of a time interval
$\xi_O(\bullet)$	Optimal energy demand in a time interval
$\xi_{lb}(\bullet)$	Lower bound of $\xi_O(\bullet)$ in a time interval
$\xi_{ub}(\bullet)$	Upper bound of $\xi_O(\bullet)$ in a time interval
$\boldsymbol{\beta}_{\mathrm{rt}}$	The tendency vector of RTP from interval 1 to current interval
θ	The degree of charging demand completeness
$\beta_{\mathrm{ct}}^{\mathrm{i}}$	The tendency vector of the *i*-th center from interval 1 to the current interval
$\boldsymbol{A}$	Coefficient vector in the dynamic linear programming algorithm
C_{max}^{i}	Maximum charging rate of the *i*-th EV
C_{min}^{i}	Minimum charging rate of the *i*-th EV
$\boldsymbol{D}$	Distance vector between RTP and price centers
$d_{r.i}$	Distance between RTP and the *i*-th price center
$E_{chg}^{i}(\bullet)$	Energy supplemented of the i-th EV in a time interval
E_{obj}^{i}	Energy demand of the i-th EV
$E_S^{min}(\bullet)$	The minimum charging demand of PVCS
$E_S^{max}(\bullet)$	The maximum charging demand of PVCS
$E_S(\bullet)$	Total energy demand of the charging station in a time interval
E_{Total}	The total amount of energy supplemented for all EVs
$\boldsymbol{E}_l^n$	Lower bounds vector from interval n to N_s
$\boldsymbol{E}_u^n$	Upper bounds vector from interval k to N_s
$E_{PV}(\bullet)$	PV energy in a time interval
$\boldsymbol{E}_O^n$	Vector of the optimal energy schedule of each time interval from interval n to N_s
$E_g(\bullet)$	Electricity purchased from the grid in a time interval
$f_r(\bullet)$	Real-time price in a time interval
$\mathbf{F}_{\mathrm{r}}$	The vector of revealed RTP
$\mathbf{F}_r^{n\to Ns}$	The newly formed RTP vector from time interval n to time interval N_s
N_s	Number of time intervals

This article has been accepted for publication in a future issue of this journal, but has not been fully edited. Content may change prior to final publication. Citation information: DOI 10.1109/TSG.2017.2693121, IEEE Transactions on Smart Grid

$N_{EV}(\bullet)$	Number of charging EVs in a time interval
Q_{PV}	The capacity of the PV system
$S^i(\bullet)$	Battery SOC of the i-th EV in a time interval
S^i_{obj}	Objective SOC of the i-th EV
t^i_0	Start charging time of the i-th EV
t^i_d	Departure time of the i-th EV
u_{ik}	Membership grade of the k-th sample that belongs to the i-th class
$\boldsymbol{U}_0$	Initial membership grade matrix
$\boldsymbol{V}$	Center matrix of m price classes
$\boldsymbol{v}_r$	Center vector of r-th price class
$\boldsymbol{v}_m$	Center vector of minimum price class
$\boldsymbol{X}$	Set of real-time price data
$y(n)$	The parabola function
z	Total cost of electricity bought from the grid

II. Introduction

Electric Vehicles (EVs) have been considered as an effective means to realize low-carbon economic transportation and have developed quickly in many countries. However, increasing EVs are expected to change the load profile greatly in distribution networks, which may cause grid reliability issues due to the less predictable large charging demands [1]. The direct integration of solar photovoltaic (PV) with EV charging infrastructure is a possible way to accommodate more clean energy, reduce carbon emissions, and alleviate peak charging loads [2]. PV can be used to produce electric energy locally wherever there is a good solar radiation resource, including urban areas that are the locations for EV applications [3] [4], such as PV-assisted Charging Stations (PVCS). For the PVCS, energy generated from the integrated PV system is only regarded as a portion of the electric energy supply, so the remaining demand must be purchased from the grid. One of the overriding concerns of the PVCS operator (PO) is to minimize the electricity purchasing costs. However, one of the main concerns of the distribution system operator (DSO) is to flatten the peak power demand.

For EV charging stations, many problems need to be studied from the different perspectives of the PO or DSO, such as coordinated charging strategy [5], the impact on grid and congestion alleviation of the grid [6, 7], the control strategy for grid active and reactive power support [8, 9], and ancillary services provision [10]. In the studies of coordinated charging strategy, the main concern is focused on how to allocate charging power effectively, from the user's perspective. In the area of impact studies, the purpose is to analyze the impact on the grid caused by large-scale EV charging activities. For the active and reactive power support area, the research is concerned with the strategy of providing voltage support. The idea of vehicle to grid (V2G) technologies is very relevant in this area. Concerning ancillary service provision, EVs may also need to work in V2G mode to provide voltage and frequency regulation services to the grid under market mechanisms. However, the lifetime and cost of EVs batteries is an issue that restricts V2G application. The main concern of this paper is to study an automatic demand response (ADR) strategy for the PVCS without V2G to improve its economic performance and reduce the charging peak load simultaneously.

DR is a valid solution to deal with both reducing electricity bill for the consumer and preventing network overloading [11] from the system perspective. DR is often a cost effective technique that can provide the flexibility required to time shift loads either through prices or incentive policies [12]. The price based DR usually contains Real-Time Prices (RTP) or Time of Use (TOU) tariffs. A comparison of TOU and RTP indicates that high resolution RTP signals will bring more benefits to power systems in terms of flattening the system load profile and reducing the peak demand as compared to TOU rates [13]. Therefore, in this paper, the focus is on RTP based DR.

Many previous works have examined DR programs with different system applications. A significant amount of the literature deals with residential DR [14-16]. In [14], in order to manage the trade-off between minimum cost and waiting time, a price prediction based optimal residential energy scheduling framework is proposed. In [15], a DR framework is proposed to control HVAC loads to reduce peak load by responding to a real-time price signal. In [16], an optimization model is proposed to adjust the consumer load in response to hourly electricity prices.

Besides residential DR, research works on EV charging strategies considering DR are also a popular topic. An automated DR mechanism for a fleet of EVs is proposed in [17], which facilitates vehicle charging to meet the needs of EVs and satisfy a load scheduling obligation. The dynamic algorithm depends only on knowledge of driving behaviors from previous similar days, and uses a simple adjusted pricing scheme to instantly assign feasible and satisfactory charging schedules to thousands of EVs in a fleet as they plug-in. An intelligent method to control EV charging loads in response to time-of-use price in a regulated market is proposed in [18]. The method is mainly based on an optimized charging model in order to minimize the charging cost, and a heuristic method is implemented to minimize the charging cost considering the relationship between the acceptable charging power of an EV battery and the state of charge (SOC). An optimization model of demand response management integrating EVs and distributed renewable generators is proposed in [19]. The costs of the local utility company and users' daily bills can be reduced concurrently. In the context of the smart grid, a DR strategy is proposed to minimize the impact of charging EVs on the distribution network in [20]. Choices of customers are taken into account and the peak demand is kept unchanged while accommodating EV charging. A comprehensive bi-level model to derive the equilibrium price of energy and reserve trading of a parking lot has been proposed considering the preferences of the PEV owners in [21]. It presented a model for the interactions of the parking lot with the market through an aggregator while considering the restrictions that the preferences of plug-in EV owners impose on its behavior.

However, the recent research on EVs or charging stations participating in DR programs are mainly concerned with charging stations without renewable energy generation systems or households with EVs. Much less attention has focused on DR for PVCS from the perspective of the PO.

Different from the aforementioned areas, an automatic demand response (ADR) strategy for PVCS from the perspective of the PO is proposed based on some previous work [22]. A comparative study is conducted between the fuzzy C-means (FCM) clustering algorithm and the K-means (KM) clustering algorithm in dealing with historic price data. Then, a new model is proposed to extract features of the historic price data and form a price vector for a particular day based on KM. The grid voltage magnitude profile is taken into consideration through a dynamic feasible energy demand region (DFEDR) model. A deduction method is proposed

This article has been accepted for publication in a future issue of this journal, but has not been fully edited. Content may change prior to final publication. Citation information: DOI 10.1109/TSG.2017.2693121, IEEE Transactions on Smart Grid

to deal with the unknown information for future time intervals considering stochastic arrival and departure times. The ADR strategy aims to minimize the electricity bill of the PVCS, while the self-consumption of PV energy and completeness of EV charging demand is guaranteed, and peak charging load is reduced. The novel contributions include the following aspects:

1) The RTP based ADR strategy for PVCS is studied without V2G, which does not harm the lifetime of the EV batteries, which is beneficial to the consumer

2) For conventional price forecasting algorithms to reach good prediction accuracy many other resources are need besides historic price data, such as: demand profiles, weather information. This information can be difficult to obtain for the PVCSs so a Dynamic Price Vector Formation Model (DPVFM) is proposed that functions only with historic price data, based on the KM clustering algorithm. The centers obtained by the KM can be designed to be updated every week or another relevant timescale. The price vector formation method is also much more simple than conventional forecasting algorithms.

3) In order to offer a proper search region for the solution of future time intervals in the DLP, a deduction method is proposed to enhance the ability of the DFEDR model to deal with upper and lower bounds of future time intervals considering stochastic arrival and departure times of EVs. Additionally, the grid voltage magnitude profile is taken into consideration to mitigate the charging impact on the grid voltage.

The content of this paper is organized as follows. Section III introduces the market conditions, typical structure, and the main function of PVCS. Section IV describes the main function of the ADR strategy, including the objective function, the DFEDR model, the DPVFM model based on the KM clustering algorithm, and the model of dynamic linear programming (DLP). The case study and related analysis of comparative case results are presented in Section V. At last, the conclusions are drawn in Section VI.

III. Market Conditions and Typical Structure of PVCS

Conventionally in most locations, users consume electricity without centralized coordination and with the same cost no matter the time. Therefore, the load curve is determined by consumers' behavior, which results in large peak loads during some certain concentrated time periods. Simultaneously, the DSO should satisfy the entire load whenever it occurs, even the short time large peak demand which appears but a few times per year. This results in large investments in expanding the generation and transmission capacity that will be idle most times during the year. With the development of smart grid technology in the future electricity distribution system and electricity market the bidirectional interaction and control between the DSO and users is enabled by advanced metering infrastructure (AMI), such as smart meters, which can provide RTP information to users [23]. Under market conditions, RTP based DR is an efficient mechanism to manage users' consumption behavior. By providing RTP to users through AMI, the DSO could realize some distributed control over users' behavior, which is preferable to peak shaving or involuntary load shedding. RTP also allow users the possibility to save money, so there is the possibility that there is a benefit for both the users and the DSO.

For the normal consumer the following problems could occur in PVCS without coordination or control: 1) the peak charging demand would be large; 2) the PV-self consumption could be very low; 3) the electricity bill could be high. However, the PO would prefer to realize coordination and control of EV charging activity, PV output and electricity purchasing activity by the potential benefits of RTP based DR under advanced electricity market conditions.

The time characteristic of PV output and the charging demand of EVs may overlap during the day. Therefore, coordinated management of EV charging activities according to PV output can result in obviously synergistic effects. In this paper, a low voltage (LV) PVCS near to commercial building is studied, and the typical structure and information flows of PV-assisted EV charging stations are shown in Fig. 1. A PV generation system that performs Maximum Power Point Tracking (MPPT) control is integrated into the system through DC/DC converter. It provides electricity to EVs during the day. The bidirectional power conversion between the grid and the PVCS is realized through the AC/DC inverter. An EV is connected to the DC bus through a charger that can regulate the charging power smoothly according to the charging command. The monitoring and control system collets information and controls other components. Parameters including control permission, departure time, and other information can be set through the human interface panel of the charger.

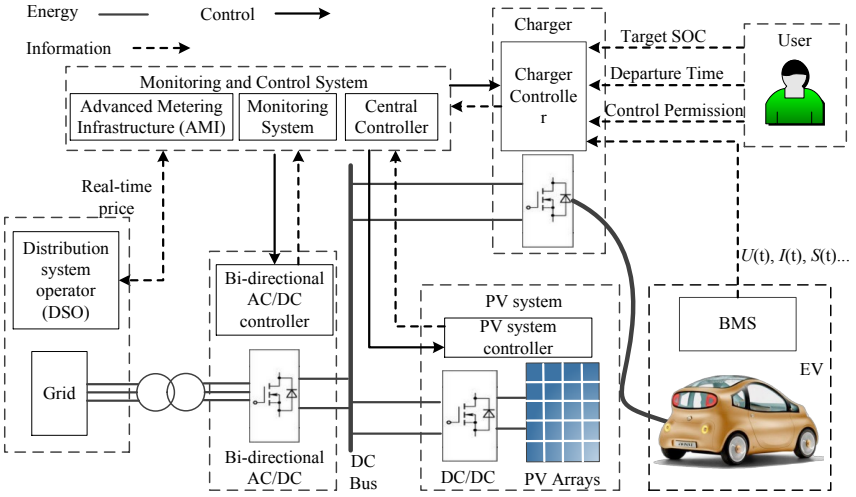

Fig. 1 Typical structure and information flows of PV-assisted EV charging station.

This article has been accepted for publication in a future issue of this journal, but has not been fully edited. Content may change prior to final publication. Citation information: DOI 10.1109/TSG.2017.2693121, IEEE Transactions on Smart Grid

In Fig.1, three roles are involved, the DSO, PO and EVs users. The DSO is not only the main power supplier, but also the policy maker, deciding the RTP policy. The PO is the operator of the PVCS who is the provider of charging service and builds its own PV generator system. EV users are the final consumer of the charging service. The PO is not only an important role in integrating PV with EV charging facilities, but also the main role in managing the charging behavior of EVs. Economics is one of the main concerns of the PO, so how the PVCS perform with RTP based DR is studied in this paper.

RTP based DR is a generalized distributed control program. RTP is like indirect control information, which could make users change their consumption behavior individually. The information interaction between the PVCS and the DSO is enabled by AMI, including RTP information. Thus, the monitoring and control system of PVCS is able to get RTP information from the DSO in cycle. There are at least two ways for PVCS to obtain RTP information from the DSO.

1) At the beginning of each cycle, the PVCS send a request message to the DSO. The DSO then sends the RTP information to the PVCS after receiving the request.

2) The DSO sends the RTP information to all users by broadcasting it.

After getting the RTP information from the DSO, the monitoring and control system collects other information from other components, such as PV output, battery SOC, and then performs optimal power allocation considering DR.

IV. Automatic Demand Response Strategy

A. Objective function

During the day, part of the charging demand of the charging station is met by the PV system and the remaining part of the charging demand is purchased from the grid. Since the price of electricity varies with time, the cost of purchasing electricity from the grid is determined by the price and energy amount. However, due to the number of EVs varies with time, it results in different energy demands at each different time interval. Therefore, for the PVCS, the objective is to satisfy the energy demand of EVs of the current time interval at a minimum cost, which are described in equations (1) and (2) as follows. The energy demand at the current time interval will be satisfied from the current time interval to the end of the charging process.

$$\min z = \sum_{n=k}^{N_S} f_r(n) E_g(n), k \in (1, N_S) \quad (1)$$

s. t.

$$E_{Total}(k) = \sum_{n=k}^{N_S} (E_{pv}(n) + E_g(n)) = \sum_{n=k}^{N_S} \sum_{i=1}^{N_{EV}(k)} E_{chg}^i(n) \quad (2)$$

where k indicates the current time interval; $E_g(n)$ is the energy purchased from the grid at time interval n; $f_r(n)$ represents the RTP of the time interval n; z indicates the total cost of purchasing energy from the grid; $E_{Total}(k)$ represents the total amount of energy demand of all EVs at the current time interval; $E_{pv}(n)$ is the energy supplied by the PV system at time interval n; N_s represents the number of time intervals; $N_{EV}(k)$ is the number of EVs at the current time interval; $E_{chg}^i(n)$ represents the charging energy of the i-th EV of time interval n.

B. Model of dynamic feasible energy demand region (DFEDR)

In order to perform DR, characteristics of energy demand should be studied to guarantee the charging demand. During the charging process, the energy supplied to all EVs in time interval *n* is the summation of the charging energy of all EVs, shown in (3).

$$E_S(n) = \sum_{i=1}^{N_{EV}(n)} E_{chg}^i(n) \quad (3)$$

where $E_S(n)$ represents the energy supplied to all EVs in time interval n.

During the charging process, the degree of charging demand completeness is defined in (4).

$$\theta = \frac{\sum_{n=1}^{N_s} \sum_{i=1}^{N_{EV}(n)} E_{chg}^i(n)}{\sum_{i=1}^{NUM} E_{obj}^i} \quad (4)$$

where θ is the degree of charging demand completeness; NUM is the total number of EVs of during the charging process; E_{obj}^i is the energy demand of the *i*-th EV.

The charging energy are supplied by the PV system and the grid together. The power balance of PVCS at time interval *n* can be described as (5).

$$E_S(n) = E_{pv}(n) + E_g(n) \quad (5)$$

Assume that C_{min}^i is the minimum charging rate of the *i*-th EV and C_{max}^i represents the maximum charging rate of *i*-th EV. C_{max}^i is a constant value determined by the charger. C_{min}^i is determined by the target State of Charge (SOC) of the EV battery, current SOC of the EV battery and charging duration of EV, calculated by (6). Then the minimum charging demand $E_S^{min}(n)$ and maximum charging demand $E_S^{max}(n)$ of the PVCS in time interval *n* can be calculated by (7) and (8) respectively.

$$C_{min}^i = (S_{obj}^i - S^i(n))/(t_d^i - t_0^i) \quad (6)$$

$$E_S^{min}(n) = \sum_{i=1}^{N_{EV}(n)} C_{min}^i \Delta t \quad (7)$$

$$E_S^{max}(n) = \sum_{i=1}^{N_{EV}(n)} C_{max}^i \Delta t \quad (8)$$

where S_{obj}^i is the target SOC of the *i*-th EV; $S^i(n)$ is the SOC in time interval *n* of the *i*-th EV; t_d^i is the departure time of the *i*-th EV; t_0^i is the arrival time of the *i*-th EV; Δt is the time length of an time interval in hours.

For the PVCS near a commercial building, most of the EVs arrive at the parking lot and start charging in the morning. However, the PV output is not sufficient to satisfy the large amount of charging demand in the morning, which results in an extra peak load to the grid and high cost. Meanwhile, the PV energy in the afternoon cannot be consumed locally and must be exported to the grid.

In order to deal with this problem, the maximum charging power should be limited in a reasonable range to reduce extra peak load and make full use of PV energy without decreasing the degree of charging completeness.

Considering the characteristic of PV output in summer, the effective start time, maximum power point time and end time of PV output is often around 6:30, 13:00 and 19:00 respectively, as shown in Fig. 2. The curve of PV output is similar to a parabola, so a parabola function is proposed to calculate the upper bound of the charging energy of each time interval.

The charging duration is from 7:00 to 18:00 and can be divided into $N_S = 660$ time intervals when a single interval is 1

This article has been accepted for publication in a future issue of this journal, but has not been fully edited. Content may change prior to final publication. Citation information: DOI 10.1109/TSG.2017.2693121, IEEE Transactions on Smart Grid

minute. Since the charging duration matches the PV output characteristics, the rectangular coordinates system is created regarding (7:00, 0 kW) as the coordinate origin (0, 0). Therefore, a parabola $y(n)$ described as (9) is generated to simulate the PV output characteristic. $y(n)$ is taken as the basic upper bound curve.

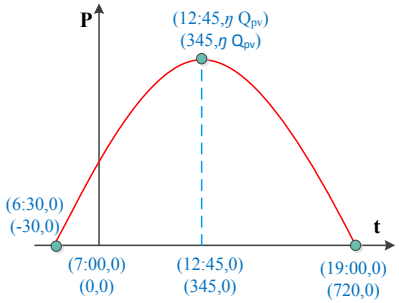

Fig. 2 Parabola model of upper bound.

$$y(n) = (an^2 + bn + c)/60, \ (n = -30,\cdots,720) \quad (9)$$

where a, b, and c are parameters tuned by characteristics of PV output. As shown in Fig. 2, three points are utilized to calculate parameters a, b, and c, which are (-30, 0), (345, ηQ_{PV}) and (720, 0), and represent (6:30, 0), (12:45, ηQ_{PV}), (19:00, 0) respectively. Q_{PV} is the capacity of the PV system; η is the typical output efficiency of the PV generation system in summer. In this paper η =0.85 and Q_{PV} =100 kW, thus a=-17/28125, b=0.4171 and c=13.06 are obtained by solving the equation.

PV output energy $E_{pv}(n)$ of time interval n, maximum energy demand $E_S^{max}(n)$ of time interval n and minimum energy demand $E_S^{min}(n)$ of time interval n are also utilized to calculate the upper bound $\xi_{ub}(n)$, as shown in (10).

1) If $E_S^{max}(n)$ is the maximum value and $y(n)$ is the second, then the upper bound equals $y(n)$. This means that setting $y(n)$ as the upper bound is large enough to guarantee the charging demand and can make full usage of PV output.
2) If $E_S^{max}(n)$ is the maximum value and $E_{pv}(n)$ is the second, then the upper bound equals $E_{pv}(n)$. It means that EVs are able to consume all of the PV output.
3) If $E_S^{max}(n)$ is less than $E_{pv}(n)$ and $y(n)$, it indicates that EVs are not able to consume all of the PV output. So charge EVs at maximum value to consume PV output as much as possible.
4) If $E_S^{min}(\mathrm{n})$ is the largest value, It means that the charging demand cannot be satisfied by PV output, so PVCS should purchase electricity from the grid. In order to cut down the peak-charging load and reduce cost, $E_S^{min}(\mathrm{n})$ is set as the upper bound to guarantee the minimum charging demand.

$$\xi_{ub}(n) = \begin{cases} y(n), E_S^{max}(\mathrm{n}) > y(n) > E_{pv}(n) > E_S^{min}(\mathrm{n}) \\ E_{pv}(n), E_S^{max}(\mathrm{n}) > E_{pv}(n) > y(n) > E_S^{min}(\mathrm{n}) \\ E_S^{max}(\mathrm{n}), \min\left(E_{pv}(n), y(n)\right) > E_S^{max}(\mathrm{n}) > E_S^{min}(\mathrm{n}) \\ E_S^{min}(\mathrm{n}), E_S^{min}(\mathrm{n}) > \max\left(E_{pv}(n), y(n)\right) \end{cases} \quad (10)$$

To satisfy the charging demand of all EVs in the PVCS, the allocated charging energy should not be lower than the minimum charging demand. Thus the lower bound $\xi_{lb}(n) = E_S^{min}(\mathrm{n})$.

However, at time interval n the information of PV output and charging demand at future times are unknown. How to determine the upper and lower bounds of time intervals $(n+1)$ to N_s is a problem. By (10), $y(n+1)$ to $y(N_s)$ can be calculated and they are regarded as the upper bound of time interval $(n+1)$ to time interval N_s. The lower bound is determined by the minimum charging demand of EVs. Because the number of EVs in future time intervals is uncertain, the actual minimum charging demand in future time intervals are also uncertain. In this paper, a deduction method is adopted to obtain an approximation of the lower bound.

Assume that all EVs are charging at the minimum charging rate and no new EVs arrive at PVCS in future time interval. Then calculate the SOC of each EV. If there are EVs meeting the target SOC, update the number of charging EVs $N_{EV}(k)$ of time interval k. Calculate the minimum charging demand of time interval k and set it as the lower bound. The flow chart is shown in Fig. 3.

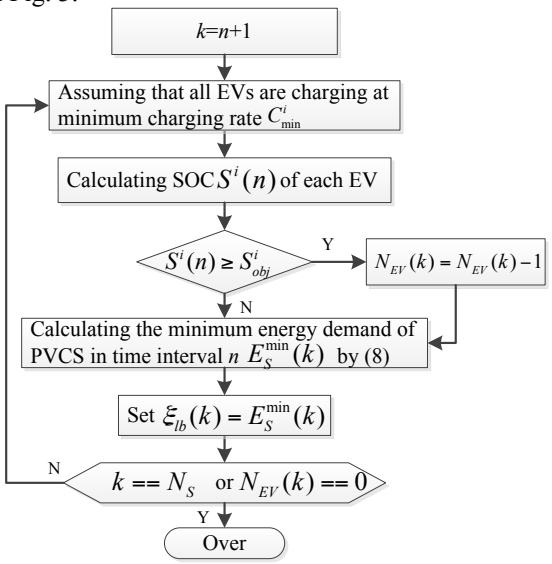

Fig. 3 Flow chart calculating the lower bound of future time interval.

Therefore, the DFEDR model in time interval n for optimal solution can be defined as (11). Because of the stochastic nature of EV charging and PV output, the DFEDR is updated in each time interval.

$$E_S(k) \in \begin{cases} [\xi_{lb}(k), \xi_{ub}(k)], k = n \\ [E_S^{min}(k), y(k)], k \in [n+1, N_S] \end{cases} \quad (11)$$

As a new type and relative large load integrating into the distribution network, it is reasonable to take the grid voltage into consideration during the charging procedure for the sake of alleviating the possible negative effects of the PVCS on grid voltage. In order to avoid deteriorating the grid voltage, an adjustment coefficient is introduced in this paper to control the upper bound and lower bound, therefore, updating the DFEDR model.

The normal operating condition of the per unit value of grid voltage magnitude is $V_g \in [0.9, 1.1]$ (this range can be set differently depends on the requirement for specific real case, such as 0.9 to 1.05) [24]. The normal grid voltage magnitude range is divided into two parts [0.9, 0.95) and [0.95, 1.1]. Thereby the adjustment coefficient ρ is defined as (12).

$$\rho = \begin{cases} 1, & V_g \in [0.95, 1.1] \\ log10^{f(V_g)}, & V_g \in [0.9, 0.95) \end{cases} \quad (12)$$

where $f(V_g)$ is a function mapping $V_g \in [0.9, 0.95)$ to [1,10) for the sake of $\rho \in [0,1)$. So function $f(V_g)$ is defined as (13)

$$f(V_g) = 1 + 180(V_g - 0.9), \quad V_g \in [0.9, 0.95) \quad (13)$$

The DFEDR model considering the grid voltage deviation is defined as (14).

This article has been accepted for publication in a future issue of this journal, but has not been fully edited. Content may change prior to final publication. Citation information: DOI 10.1109/TSG.2017.2693121, IEEE Transactions on Smart Grid

$$E_S(k) \in \begin{cases} [\max(\rho\xi_{lb}(k), E_{pv}(k)), \max(\rho\xi_{ub}(k), E_{pv}(k))] \\ ,k = n \\ [(\rho E_S^{min}(k), \rho y(k))], k \in [n+1, N_S] \end{cases} \quad (14)$$

Therefore, with the adjustment coefficient ρ the DFEDR model can be used to curtail the charging power reasonably if the grid voltage exceeds the normal range.

C. Dynamic price vector formation model (DPVFM)

RTP is the most important outside command information for DR, which varies with time in each period and each day. Although RTP varies stochastically, the RTP of most days tends to follow a similar pattern. Many research works have been conducted to deal with these kinds of randomness based on smart prediction algorithms [25-27]. In this paper, the clustering algorithm is applied to deal with the stochastic RTP features.

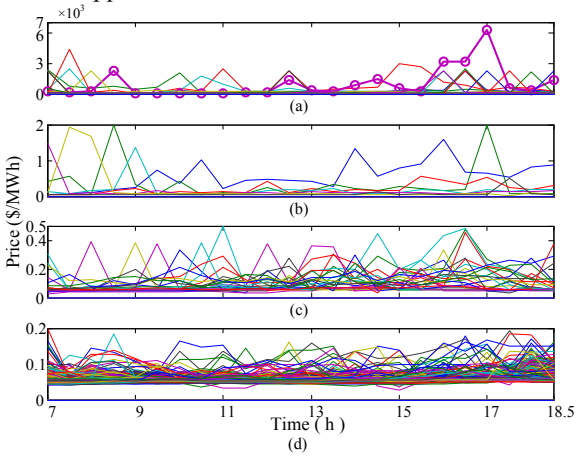

Fig. 4 One year historic RTP data from 7:00 through 18:30. (Subplot (a) represents days on which the maximum RTP value is larger than 2000 $/MWh; subplot (b) provides the days on which the maximum RTP value is larger than 500 $/MWh but less than 2000 $/MWh; subplot (c) shows the days on which the maximum RTP value is larger than 200 $/MWh but less than 500 $/MWh; subplot (d) illustrates the days on which the maximum RTP value is less than 200 $/MWh.)

Historical data of one year of RTP (in 30 minutes intervals) is utilized to depict the range of variations that may occur and was obtained from the Australia Energy Market Operator (AEMO) [28]. As shown in subfigure (d) of Fig. 4, most days with the RTP less than 200 $/MWh (the number is 315 days). There are 24 days with maximum RTP value between 200 $/MWh and 500 $/MWh (see subfigure (c)) and 26 days with price spikes larger than 500 $/MWh (see subfigure (b) and (a)). RTP varies stochastically and the price spikes appear at different times, so clustering algorithms have been utilized to capture the features of RTP in this paper.

There are many clustering algorithms that have been applied to different applications. Considering the application of this paper and computational complexity of algorithms, fuzzy C-means (FCM) and K-means (KM) algorithm are utilized.

➢ Application of the FCM clustering algorithm

In this part the FCM algorithm is taken into consideration, the steps are as follows.

Assume that $\boldsymbol{X}$ is the RTP dataset, $\boldsymbol{V}$ is the center matrix of r classes. They can be described as (15) and (16) respectively.

$$\boldsymbol{X} = \{x_1, x_2, \cdots, x_n\} \quad (15)$$

$$\boldsymbol{V} = \{v_1, v_2, \cdots, v_r\} \quad (16)$$

where x_n is the price vector of n-th day, v_r is the center vector of r-th class.

Assume that u_{ik} is the membership grade of that the k-th sample belongs to the i-th class.

$$0 \le u_{ik} \le 1, \sum_{i=1}^{r} u_{ik} = 1 \quad (17)$$

Define the objective function:

$$min\, J(\boldsymbol{U}, \boldsymbol{V}) = \sum_{k=1}^{n}\sum_{i=1}^{r} (u_{ik})^2 (d_{ik})^2 \quad (18)$$

where $d_{ik} = \|x_{k-} v_i\|$ is Euclidean distance.

The steps to solve the fuzzy C-means clustering problem are as following:

1) Select the value of r and the initial membership grade matrix $\boldsymbol{U}_0$, set the iteration count $I = 0$;

2) Calculate the center $\boldsymbol{V}$ by (20);

$$v_i^{(l)} = \sum_{k=1}^{N} \left(u_{ik}^{(l)}\right)^2 x_k \Big/ \sum_{k=1}^{N} \left(u_{ik}^{(l)}\right)^2, (i = 1, \dots, m) \quad (19)$$

3) Correct the membership grade matrix;

$$u_{ik}^{(l+1)} = 1 \Big/ \sum_{j=1}^{r} \left(d_{ik}/d_{jk}\right)^2, \forall i, \forall k \quad (20)$$

4) If $\varepsilon > 0$, calculating till $max\{|u_{ik}^{l} - u_{ik}^{l-1}|\} < \varepsilon$, else, set $l = l + 1$ and jump to step 2).

5) If $u_{jk} = max\{u_{ik}\} > 0.5$, x_k belongs to j-th class.

Set $r = 7$. Define $\mathbf{V}_c$ as (21), it is the matrix consisting of the center vectors of 7 price classes.

$$\begin{cases} \mathbf{V}_c = [\mathbf{v}_1 \ \mathbf{v}_2 \ \cdots \ \mathbf{v}_7] \\ \mathbf{v}_i = [v_{i,1}, v_{i,2}, \cdots, v_{i,N_s}]^T, \end{cases} (i = 1,2,\cdots,7) \quad (21)$$

where $\mathbf{v}_i$ is the center vector of the i-th class.

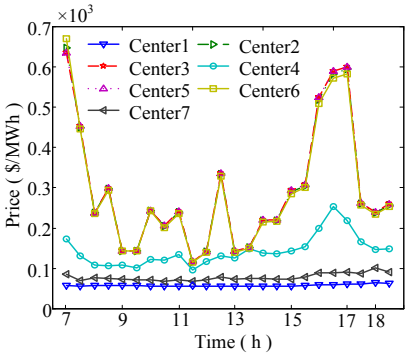

Fig. 5 7 centers obtained by the FCM algorithm.

The 7 centers obtained by FCM are shown in Fig. 5. Four of the 7 centers almost coincide, which indicates that FCM can easily be affected by the largest value of each time point. Compared with Fig. 3, the FCM does extract some features of historic price data, but the largest variation features of each time point are clustered to one class, which is much like the envelopes. This is inconsistent with the historic data presented.

➢ Application of KM clustering algorithm

In this part the KM clustering algorithm is utilized. The dataset of RTP and centers are defined in (15) and (16), respectively. The objective is to minimize the distance between the center points and data points, shown in (22).

$$min\, J(\boldsymbol{V}) = \sum_{i=1}^{r}\sum_{j=1}^{n_i} \|x_j - v_i\|^2 \quad (22)$$

where r is the number of cluster center, n_i is the number of data points in i-th cluster.

The steps are as follows:

1) Select the number r of clustering centers.

2) Calculate the distance $\|x_j - v_i\|^2$ between each data point and cluster centers.

This article has been accepted for publication in a future issue of this journal, but has not been fully edited. Content may change prior to final publication. Citation information: DOI 10.1109/TSG.2017.2693121, IEEE Transactions on Smart Grid

3) Assign the data point to the cluster center whose distance to the center is the minimum of all the cluster centers.

4) Recalculate the new cluster center by (23)

$$v_i = \left(\frac{1}{n_i}\right)\sum_{j=1}^{n_i} x_j \tag{23}$$

5) Recalculate the distance between each data point and the newly obtained centers.

6) Repeat 4) and 5), until the cluster centers converge to constant values.

The same as in FCM, set $r = 7$ and define $\mathbf{V}_c$ as (21).

The 7 centers obtained by KM are shown in Fig. 6. Compared with Fig. 5, more features are extracted from the historic RTP data. No centers coincide with each other and no envelope phenomenon occurs. The results are closer to the original feature shown in Fig. 4. So, the KM algorithm is regarded as the foundation of the DPVFM. In order to get more features from historic data, centers number r is set to 20 in this paper.

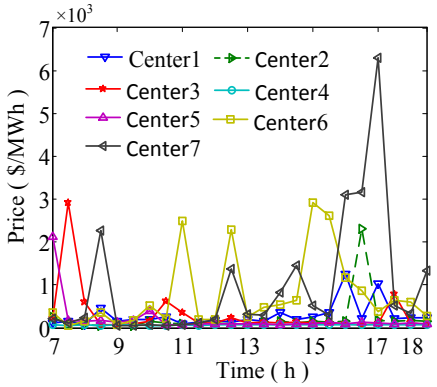

Fig. 6 7 centers obtained by KM algorithm.

➢ Dynamic price vector formation model

Let $\mathbf{F}_r$ represent the vector of revealed RTPs after time interval n, $f_r(n)$ represents the price of time interval n, as shown in (24).

$$\mathbf{F}_r = [f_r(1)\ f_r(2)\ \cdots\ f_r(n)], (n \in [1, N_s]) \tag{24}$$

Define $\boldsymbol{\beta}_{rt}$ as the tendency vector of RTPs at time interval n, $\boldsymbol{\beta}_{ct}^{i}$ as the tendency vector of the i-th center, shown in (25) and (26) respectively.

$$\begin{cases} \boldsymbol{\beta}_{rt} = [\beta_r(1)\ \beta_r(2)\ \cdots\ \beta_r(n)] \\ \beta_r(1) = f_r(1) \\ \beta_r(i) = \frac{(f_r(i) - f_r(i-1))}{f_r(i)} \end{cases}, \begin{pmatrix} n \in [1, N_s] \\ i \in [2, n] \end{pmatrix} \tag{25}$$

$$\begin{cases} \boldsymbol{\beta}_{ct}^{i} = [\beta_c^i(1)\ \beta_c^i(2)\ \cdots\ \beta_c^i(n)] \\ \beta_c^i(1) = v_{i,1} \\ \beta_c^i(j) = \frac{(v_{i,j} - v_{i,j-1})}{v_{i,j}} \end{cases}, \begin{pmatrix} n \in [1, N_s] \\ i \in [1,20] \\ j \in [2, n] \end{pmatrix} \tag{26}$$

Therefore, the distance vector $\boldsymbol{D}$ between the RTP tendency and 7 centers tendency can be defined as (27).

$$\begin{cases} \boldsymbol{D} = [d_{r.1}\ \ d_{r.2}\ \cdots\ \ d_{r.7}] \\ d_{r.i} = \sqrt{\sum_{j=1}^{n}(\beta_r(j) - \beta_c^i(j))^2} \end{cases}, \begin{pmatrix} n \in [1, N_s] \\ i \in [1,7] \end{pmatrix} \tag{27}$$

Let $\mathbf{F}_r^{n \to N_S}$ represent the newly formed RTP vector of time interval n. Then $\mathbf{F}_r^{n \to N_S}$ is formed as (28) based on the distance vector $\boldsymbol{D}$.

$$\mathbf{F}_r^{n \to N_S} = [f_r(n)\ \ v_{i,n+1}, v_{i,n+2}, \cdots, v_{i,N_S}],\ d_{r.i} \in min(\boldsymbol{D}) \tag{28}$$

D. Model of DLP

The flow chart for solving for the optimal solution of the DR problem in time interval n is shown in Fig. 7.

The charging process is stochastic, not only the PV output, RTP, and charging demand, but also the number of time intervals varies from N_s to 0, which results in the dimensions of variables varying with the time interval. In order to deal with the stochastic features of the charging process, each time interval is regarded as a state and the DR problem is modeled based on DLP, shown in (29).

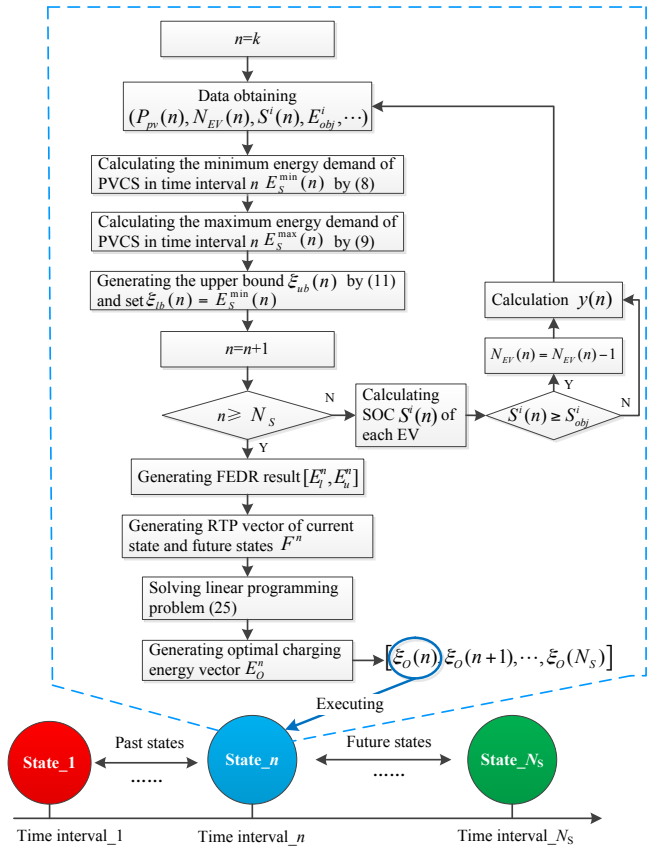

Fig. 7 Flow chart of figuring out optimal charging energy vector based on DLP.

$$\begin{cases} min\ z = \mathbf{F}_r^{n \to N_S} \boldsymbol{E}_O^n, 1 \le n \le N_s \\ \boldsymbol{A}\boldsymbol{E}_O^n = E_S(n \to N_s) \\ \xi_{lb}(k) \le \xi_O(k) \le \xi_{ub}(k), n \le k \le N_s \end{cases} \tag{29}$$

where the length of $\mathbf{F}_r^{n \to N_S}$ varies with time from N_s to 0; $\boldsymbol{E}_O^n$ is the vector of optimal energy allocation results of the PVCS from time interval n to N_s, shown as (30), $\xi_O(n)$ is the optimal energy allocation of PVCS in time interval n. The length of $\boldsymbol{E}_O^n$ varies with time from N_s to 0. $\boldsymbol{A}$ is the coefficient vector of the equality, A=[1， 1， …， 1， 1], and the length of $\boldsymbol{A}$ varies with time from N_s to 0. $E_S(n \to N_s)$ is the total energy demand of PVCS from time interval n to time interval N_s.

$$\boldsymbol{E}_O^n = [\xi_O(n)\ \ \xi_O(n+1) \cdots\ \xi_O(N_s)\ ]^T \tag{30}$$

The energy purchased from the grid at interval n is calculated by (31). If PV output is sufficient, $E_g(n)$ is negative. It indicates that the PVCS selling energy to the grid. Otherwise, $E_g(n)$ is positive, and the PVCS purchases energy from the grid.

$$E_g(n) = \xi_O(n) - E_{PV}(n) \tag{31}$$

where $E_g(n)$ is the energy purchased from the grid.

To calculate the vector of optimal energy allocation the DFEDR model is designed to provide the feasible region. It is important in satisfying the energy demand and alleviating extra peak charging load. Assume that $\boldsymbol{E}_l^n$ is the vector of lower bound and $\boldsymbol{E}_u^n$ is the vector of upper bounds, shown as (32) and (33) respectively. The length $\boldsymbol{E}_l^n$ and $\boldsymbol{E}_u^n$ are both vary from N_s to 0.

This article has been accepted for publication in a future issue of this journal, but has not been fully edited. Content may change prior to final publication. Citation information: DOI 10.1109/TSG.2017.2693121, IEEE Transactions on Smart Grid

$$\boldsymbol{E}_l^n = [\xi_{lb}(n) \quad \xi_{lb}(n+1) \cdots \xi_{lb}(N_s)\,] \tag{32}$$

$$\boldsymbol{E}_u^n = [\xi_{ub}(n) \quad \xi_{ub}(n+1) \cdots \xi_{ub}(N_s)\,] \tag{33}$$

where $\xi_{lb}(n)$ represents the lower bound of time interval n; $\xi_{ub}(k)$ indicates the upper bound of time interval n.

V. Case Studies

A. Parameters of simulation

In the following simulations, the rated capacity of the PV system is 100 kW, the irradiance data is obtained from the Measurement and Instrumentation Data Center (MIDC) of the National Renewable Energy Laboratory (NREL) online [29]. The number of EVs is 60, and the parameters of the EVs are shown in Table I.

The initial SOCs of 60 EVs are generated randomly and shown in Fig. 8. The start time, departure time and charging duration of EVs are obtained from an actual parking lot, shown in Fig. 9. The simulation runs from 7:00 to 18:00 with 660 time intervals and the length of each time interval is 1 minute. The actual prices and the predicted prices of 7 consecutive days are shown in Fig. 10.

TABLE I
Parameters of PV-assisted charging station

Objective SOC	*capacity Ah*	*Capacity kWh*	*Maximum charging rate*	*Rated voltage*
0.85	70	22.4	0.223	320V

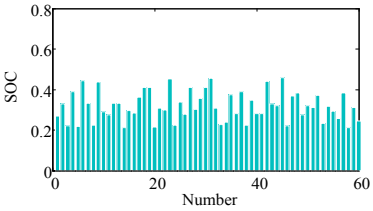

Fig. 8 Initial SOC of 60 EVs.

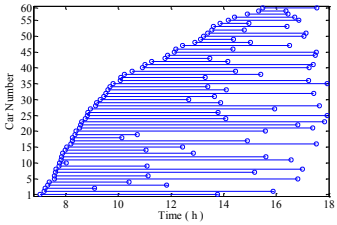

Fig. 9 Start time, departure time and charging duration of 60 EVs.

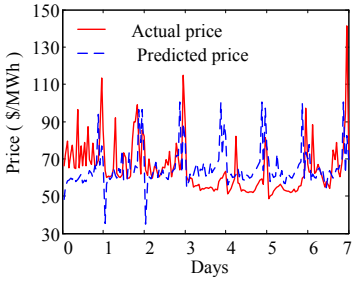

Fig. 10 The detailed information of RTP.

B. Analysis and comparison results

To better analyze the validity of the proposed ADR strategy, five comparative cases are considered as the follows:

Case 1: Uncontrolled Charging Strategy of a typical day. EVs are charged with constant power as soon as they arrive, until the SOCs reach the target values.

Case 2: The DR strategy is formulated as a day-ahead horizon optimization problem. The day-ahead price is forecasted by the BPNN algorithm proposed in [25]. The charging demand is estimated at the beginning and the maximum charging power is bounded by the parabola proposed in this paper. Finally, the charging power is allocated according to the day-ahead optimal schedule and the actual charging demand by the earliest deadline first (EDF) method, which was shown to be the best in terms of missed requirement amounts in [30].

Case 3: The DR strategy is based on a real-time horizon. The price is forecasted at each time interval and the forecasting window is 10 time slots. The charging demand is calculated at each time interval and the maximum charging power is bounded by the parabola proposed in this paper. Finally, the charging power is allocated by the EDF method.

Case 4: The DR strategy is based on predicted price. The prices of seven consecutive days is predicted by the BPNN algorithm [25], and the DLP and DFEDR, without considering the voltage deviation, for seven consecutive days are conducted.

Case 5: In the proposed ADR strategy, all of the parameters and conditions are the same as in Case 4, except that voltage deviation is considered in the DFEDR and the DPVFM model is utilized to form the price vectors of seven consecutive days.

The simulation results of five cases are shown in Figs. 11 - 15, and some indices of performance are shown in Table II.

In Case 1, since the charging power of EVs cannot be controlled, the large peak load comes along with the increasing number of EVs. In Fig. 11, the peak occurs about 8:00-10:00. During this period, the charging power is much larger than PV output, which means that most of the charging power needs to be supplied by the power grid.

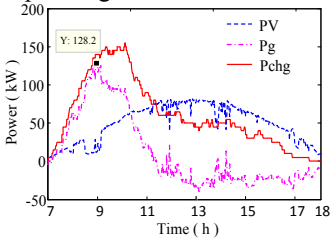

Fig. 11 Simulation result of Case 1(UCS).

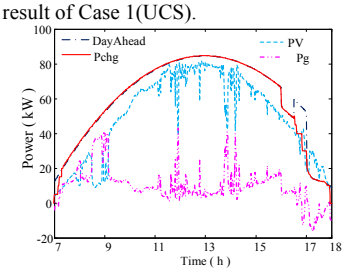

Fig. 12 Simulation results of the first day in Case 2.

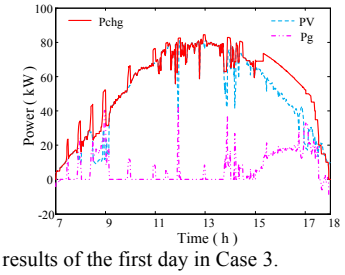

Fig. 13 Simulation results of the first day in Case 3.

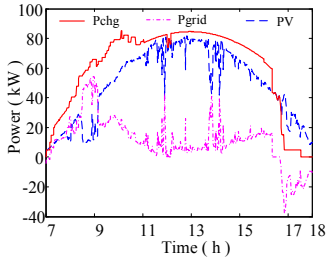

Fig. 14 Simulation results of the first day in Case 4.

This article has been accepted for publication in a future issue of this journal, but has not been fully edited. Content may change prior to final publication. Citation information: DOI 10.1109/TSG.2017.2693121, IEEE Transactions on Smart Grid

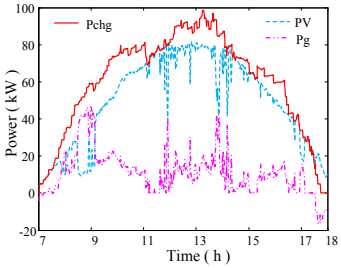

Fig. 15 Simulation results of the first day in Case 5.

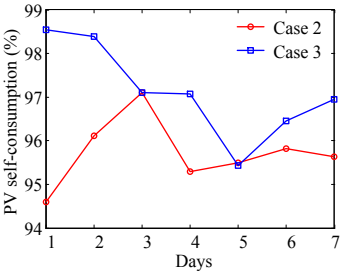

Fig. 16 PV self-consumption Comparison between Case 4 and Case 5.

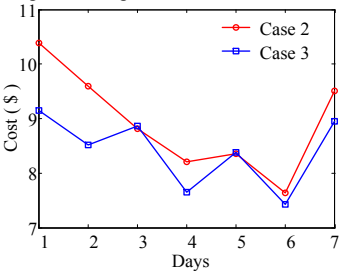

Fig. 17 Cost comparison between Case 4 and Case 5.

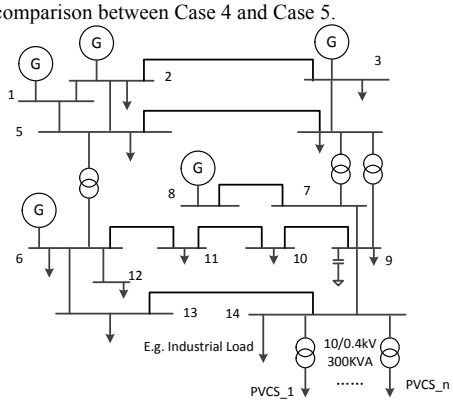

Fig. 18 Simulation system topology.

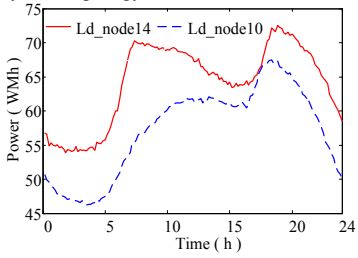

Fig. 19 Load profile of node 10 and node 14.

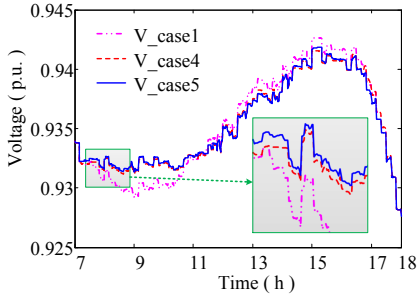

Fig. 20 Voltage profile of node 14.

The simulation results of Case 2 are shown in Fig. 12. In Case 2, the day-ahead optimal schedule is designed for seeking the global solution. The charging demand and the charging load profile can be estimated within a certain error. But the start charging time and departure time of EVs are stochastic, which would affect the power allocation. As shown in Fig 12, at the beginning and around 16:30, the day-ahead scheduled power is larger than the actual demand. Therefore, the actual charging power cannot follow the day-ahead schedule.

The simulation results of Case 3 are shown in Fig. 13. In Case 3, it is supposed to cope with the variation of variables in a real-time regulation manner. However, due to the limitation of unknown information in the future hours, the schedule is only an optimal solution in a real-time window not a global one. So during the optimization window peak charging load would appear at those time slots with lower price (such as 7:00 to 9:00) or with larger charging demand (such as 15:30 to 17:30).

In Case 4, at about 11:00 the number of charging EVs reaches the maximum value and the PV energy is not enough to fulfill this demand. In order to guarantee the degree of charging completeness, the lower bound calculated by the DFEDR model is larger than the proposed parabola value. According to equation (10), the upper bound equals the lower bound. In Fig. 10, according to the forecasted value of the first day, the price before 16:30 is much lower, which results in charging power following the upper bound before 16:30. Therefore most of the EVs are scheduled to finish charging before 16:30, except those EVs who arrive at the PVCS at a late time and do not have enough time to finish charging before 16:30, as seen in Fig. 14. Therefore, the self-consumption of PV energy is decreased. Moreover, the actual price of the first day is larger than the predicted price, which results in a high cost ($10.39).

The results of Case 5 are shown in Fig. 15, with the charging power is following the upper bound before 11 AM. The reason is the same as in Case 2. Because the price is high and PV energy is sufficient to satisfy the minimum charging demand between 11:00 to 12:00, charging power follows PV output. After 12:00 PM, charging power follows the upper bound, PV output and the lower bound dynamically due to the dynamic price. Especially after 15:00, the charging power follows the lower bound and PV output to avoid higher costs.

TABLE II
Indices Comparison of 5 cases

Indices	*Case 1*	*Case 2*	*Case 3*	*Case 4*	*Case 5*
θ (%)	93.08	90.8	85.24	92.7	92.5
Cost ($)	17.98	8.42	4.92	10.39	8.98
Purchased energy (kWh)	269.4	116.9	70.3	144.7	125.9
PV self-consumption (%)	73.48	98.49	99.75	95.6	98.94
Peak load (kW)	128.2	43.03	43.03	54.13	46.78

Case 1 is the regular strategy and is regarded as a benchmark here. Comparing the results of the five cases in Table II, the degree of charging demand completeness of Case 1 is the highest but does not reach 100%. This is because several EVs do not have enough time to finish charging, even under perfect conditions. Due to the lack optimal scheduling, the cost and the peak load is the highest but the PV self-consumption is the lowest.

The cost of Case 3 is the lowest but the degree of charging demand completeness is also the lowest. Because the real-time optimal schedule is not within the global horizon to guarantee the charging demand due to the limited optimization window and limited information. The PV self-consumption is the highest because the charging schedule is adjusted according to the real-time PV output and charging demand.

Case 2, Case 4, and Case 5 are aimed at obtaining the optimal solution in the global horizon, so the degree of charging demand completeness is higher than that in Case 3. The cost is also reasonable for satisfying charging demand. The reason that the degree of charging demand completeness of Case 2 is lower than that in Case 4 and Case 5 is that the day-ahead strategy in Case 2 lacks of real-time adjustment.

In order to compare the performance of Case 4 and Case 5, the comparative indices of seven consecutive days are shown in Fig. 16 – Fig. 17. Both price prediction based DR and the proposed ADR strategy present good performance in PV self-consumption promotion and cost reduction under different RTP conditions. But the proposed ADR is more stable than the price prediction based DR. This is because the KM algorithm has an excellent performance in price feature extraction. Moreover, the proposed ADR strategy is better in alleviating voltage deterioration, as seen in Fig. 20.

To evaluate the impact on voltage magnitude profile and the voltage deterioration alleviation performance of proposed DFEDR, the IEEE 14-bus system is regarded as the basic network structure, as shown in Fig. 18. The load profile on node 10 and node 14 are shown in Fig. 19 and there are 15 PVCS integrated into the system at node 14. The voltage profile of Case 1, Case 4, and Case 5 are shown in Fig. 20. In Case 1, the charging activity is uncontrolled, so the impact on the voltage magnitude profile is greater than that in the other two cases. Because the voltage magnitude is taken into consideration in the DFEDR model, the peak charging load is reduced (see Table II). So the voltage magnitude profile of Case 3 is better than it in Case 2.

Comparing Case 5, Case 2, and Case 3, the proposed ADR strategy combines the advantages of global optimization and real-time adjustment.

Comparing Case 5 and Case 4, the DPVFM presents good performance in dealing with the stochastic RTP, which lays a solid foundation for the proposed ADR strategy to present a more stable performance in cost reduction and PV self-consumption improvement.

The results of the five cases show that the proposed ADR strategy has good performance in coping with the compromises among the degree of charging demand completeness, electricity cost, PV self-consumption, and voltage magnitude deterioration alleviation.

VI. Conclusions

The RTP based ADR strategy for PVCS is studied without V2G so as to will not harm the lifetime of EV batteries, a more realistic and practical assumption than many previous studies. It aims to minimize the cost of electricity purchased from the grid, while the self-consumption of PV energy and completeness of EV charging demand are both guaranteed, and the impact on the distribution network is reduced as well. The proposed ADR strategy is able to adapt to RTP and voltage magnitude variations because of the DPVFM and DFEDR model. The DPVFM model based on KM clustering algorithm is proposed to generate a price vector without forecasting algorithms. The DFEDR model guarantees charging demand and mitigates the peak load effectively. The comparative simulation results show that the proposed ADR strategy works well in reducing electricity costs, improving PV self-consumption, and mitigating the impacts on grid voltage magnitude.

VII. References

[1] Daehyun Ban, George Michailidis, Michael Devetsikiotis. "Demand Response Control for PHEV Charging Station by Dynamic Price Adjustments," Innovative Smart Grid Technologies (ISGT), 2012 IEEE PES, pp. 1-8, 2012.

[2] Y. M. Wi, J. Uk Lee, S. K. Joo, "Electric Vehicle Charging Method for Smart Homes/Buildings with a Photovoltaic System," *IEEE Trans on Consumer Electron*, vol.59, pp. 323-328, May, 2013.

[3] Manuela Sechilariu, Baochao Wang, Fabrice Locment. "Building Integrated Photovoltaic System with Energy Storage and Smart Grid Communication", *IEEE Trans. Ind Electron*, vol. 60, pp. 1607-1618, 2013.

[4] F. Marra, G.Y. Yang, C. Traeholt, "EV Charging Facilities and Their Application in LV Feeders with Photovoltaics." *IEEE Trans. Smart Grid*, vol. 4, pp: 1533-1540, 2013.

[5] N. Liu, Q. Chen, J. Liu, X. Y. Lu, P. Li, J. Y. Lei and J. H. Zhang. "A Heuristic Operation Strategy for Commercial Building Microgrids Containing EVs and PV System," *IEEE Trans. Ind Electron*, vol.62, pp, 2560-2570, 2015.

[6] Else Veldman, Remco A. Verzijlbergh. "Distribution Grid Impacts of Smart Electric Vehicle Charging From Different Perspectives," *IEEE Trans. Smart Grid*, vol. 6, pp. 333-342, 2015.

[7] C. C. Shao, X. F. Wang, M. Shahidehpour, X. L. Wang and B. Y. Wang, " Partial Decomposition for Distributed Electric Vehicle Charging Control Considering Electric Power Grid Congestion," *IEEE Trans. Smart Grid*, vol. PP, pp. 1-1, 2016.

[8] S. Deilami, Amir S. Masoum, Mohanmmad A. S. Masoum, et al. "Real-Time Coordination of Plug-In Electric Vehicle Charging in Smart Grid to Minimize Power Losses and Improve Voltage Profile," *IEEE Trans. Smart Grid*, vol. 2, pp. 456-467, 2011.

[9] J. Hu, S. You, M. Lind, J. Ostergaard. "Coordinated Charging of Electric Vehicles for Congestion Prevention in the Distribution Grid," *IEEE Trans. Smart Grid*, vol. 5, pp. 703-711, 2014.

[10] E. Sortomme, Mohamed A. El-Sharkawi. "Optimal Scheduling of Vehicle-to-Grid Energy and Ancillary Services," *IEEE Trans. Smart Grid*, vol. 3, pp. 351-359, 2012.

[11] C. Vivekananthan, Y. Mishra, G. Ledwich. "Demand Response for Residential Appliances via Customer Reward Scheme," *IEEE Trans. Smart Grid*, vol. 5, pp. 809-820, 2014.

[12] F. Wang, H. Xu, T. Xu, K. Li, M. Shafie-khah, J.P.S. Catalão. "The values of market-based demand response on improving power system reliability under extreme circumstances," *Appl. Energy*, vol. 193, pp. 220-231, 2017.

[13] S. Borenstein, M. Jaske, and A. Rosenfeld, "Dynamic pricing, advanced metering and demand response in electricity markets," Center for the Study of Energy Markets, UC Berkeley, 2002.

[14] A.-H. Mohsenian-Rad, A. Leon-Garcia, "Optimal residential load control with price prediction in real-time electricity pricing environments," *IEEE Trans. Smart Grid*, vol. 1, pp. 120–133, 2010.

[15] J. H. Yoon, R. Baldick, A. Novoselac, "Dynamic Demand Response Controller Based on Real-Time Retail Price for Residential Buildings," *IEEE Trans. Smart Grid*, vol. 5, pp. 121–129, 2014.

[16] A. J. Conejo, J. M. Morales, and L. Baringo, "Real-time demand response model," *IEEE Trans. Smart Grid*, vol. 1, pp. 236–242, 2010.

[17] N. Taheri, R. Entriken, Y Y. Ye, "A Dynamic Algorithm for Facilitated Charging of Plug-In Electric Vehicles," *IEEE Trans. Smart Grid*, vol. 4, pp. 1772-1779, 2013.

[18] Y. Cao, S. Tang, C. Li, et al. "An Optimized EV Charging Model Considering TOU Price and SOC Curve," *IEEE Trans. Smart Grid*, vol. 3, pp. 388-393, 2012.

[19] T. Zhao, Y. Peng, A. Nehorai, "An Optimal and Distributed Demand Response Strategy with Electric Vehicles in Smart Grid," *IEEE Trans. Smart Grid*, vol. 5, pp. 861-869, 2014.

[20] S. Shao, M. Pipattanasomporn, S. Rahman, "Grid Integration of Electric Vehicles and Demand Response with Customer Choice," *IEEE Trans. Smart Grid*, vol. 3, pp. 543-550, 2012.

[21] N. Neyestani, M. Y. Damavandi, M. Shafie-khah, A. G. Bakirtzis and J. P. S. Catalão, " Plug-in Electric Vehicles Parking Lot Equilibria with Energy and Reserve Markets," *IEEE Trans. Power Syst*, vol. PP, pp. 1-1, 2016.

[22] Q. Chen, N. Liu, Y. Cui, X. Lin J. Zhang. "Real-time Energy Management Algorithm for PV-assisted Charging Station Considering Demand Response," *2015 IEEE Power & Energy Society General Meeting*, pp, 1-5, 2015.

[23] A. P. S. Meliopoulos, G. Cokkinides, R. Huang, E. Farantato, S. Choi, Y. Lee, and X. Yu, "Smart grid technologies for autonomous operation and control," *IEEE Trans. Smart Grid*, vol. 2, no. 1, pp. 1–10, Mar. 2011.

[24] N. Leemput, F. Geth, J. V. Roy, et al. "Impact of Electric Vehicle On-Board Single-Phase Charging Strategies on a Flemish Residential Grid," *IEEE Trans. Smart Grid*, vol. 5, no. 4, pp. 1815–1822, Jul. 2014.

[25] B. Yi, W. Liu. "Research on Prediction Methods of Residential Real Estate Price Based on Improved BPNN," *2016 International Conference on Smart Grid and Electrical Automation (ICSGEA)*, Aug. 2016.

[26] F. Wang, Z. Mi, S. Su, H. Zhao. "Short-Term Solar Irradiance Forecasting Model Based on Artificial Neural Network Using Statistical Feature Parameters," *Energies*, vol. 5, pp. 1355-1370, 2012.

[27] F. Wang, Z. Zhen, Z. Mi, H. Sun, S. Su, G. Yang. "Solar irradiance feature extraction and support vector machines based weather status pattern recognition model for short-term photovoltaic power forecasting," *Energy Build*, vol. 86, pp. 427-438, 2015.

[28] [Online]. Available: http://www.aemo.com.au/Electricity/Data/Price-and-Demand/Aggregated-Price-and-Demand-Data-Files/Aggregated-Price-and-Demand-2011-to-2015.

[29] National Renewable Energy Laboratory (NREL). (2014, Sep. 20). "NREL: MIDC/Oahu Irradiance Grid," [Online]. Available: http://www.nrel.gov/midc/oahu_archive/.

[30] J. Huang, V. Gupta, and Y.-F. Huang, "Scheduling algorithms for PHEV charging in shared parking lots," in Proc. Amer. Control Conf. (ACC), Montreal, QC, Canada, Jun. 2012, pp. 276–281.

Qifang Chen (S'14) received the B.S. and M.S. degrees in communication and electric engineering from Xiangtan University, Hunan, China, in 2010 and 2013, respectively. Currently, he is pursuing the Ph.D. degree in the School of Electrical and Electronic Engineering of North China Electric Power University, Beijing, China. He is also a visit Ph.D. student with the Department of Electrical and Computer Engineering, University of Illinois at Urbana-Champaign, Urbana, IL 61801, USA. His research interests include demand side energy management, electric vehicle charging station and micro grids.

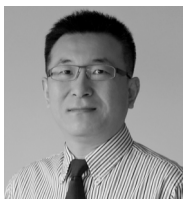

Fei Wang (M'09) received the B.S. degree from Hebei University, Baoding, China in 1993, the M.S. and Ph.D. degrees in electrical engineering from North China Electric Power University, Baoding, China, in 2005 and 2013, respectively. Currently, he is a visiting Professor with the Department of Electrical and Computer Engineering, University of Illinois at Urbana-Champaign, Urbana, IL, USA, also with the Department of Electrical Engineering at North China Electric Power University, Baoding, China, and also with the State Key Laboratory of Alternate Electrical Power System with Renewable Energy Sources. He was a researcher with the Department of Electrical Engineering at Tsinghua University, Beijing, China from 2014 to 2016. He was the recipient of the 2014 Natural Sciences Academic Innovation Achievement Award of Hebei Province and the 2014 Outstanding Doctoral Dissertation Award of North China Electric Power University. His research interests include power system modeling, simulation and optimization; renewable energy power generation, load and electricity price forecasting; demand response; electricity market; micro-grid operation and control.

Bri-Mathias Hodge (M'09, SM'17) received the B.S. degree in chemical engineering from Carnegie Mellon University in 2004, the M.S. degree from the Process Design and Systems Engineering Laboratory of Å bo Akademi, Turku, Finland, in 2005, and the Ph.D. degree in chemical engineering from Purdue University in 2010. He is currently the Manager of the Power System Design and Studies Group at the National Renewable Energy Laboratory (NREL), Golden, CO. His current research interests include energy systems modeling, simulation, optimization, and wind power forecasting.

Jianhua Zhang (M'09) was born in Beijing, China, in 1952. He received the M.S. degree in electrical engineering from North China Electric Power University, Beijing, China, in 1984. He was a Visiting Scholar with the Queen's University, Belfast, U.U., from 1991 to 1992, and was a Multimedia Engineer of Electric Power Training with CORYS T.E.S.S., France, from 1997 to 1998. Currently, he is a Professor and Head of the Transmission and Distribution Research Institute, North China Electric Power University, Beijing. He is also the Consultant Expert of National "973" Planning of the Ministry of Science and Technology. His research interests are in power system security assessment, operation and planning, and micro-grid. Prof. Zhang is an IET Fellow and a member of several technical committees.

Zhigang Li (S'13, M'16) received the B.S and Ph.D. degrees in electrical engineering from Tsinghua University, Beijing, China, in 2011 and 2016, respectively. He is currently an Associate Professor with the School of Electric Power, South China University of Technology, Guangzhou, China. He was a Visiting Scholar at the Illinois Institute of Technology, Chicago, IL, USA, and the Argonne National Laboratory, Argonne, IL, USA, from 2014 to 2015. His research interests include renewable energy integration, power system optimization, and integrated energy systems.

Miadreza Shafie-khah (S'08, M'13) received the M.Sc. and Ph.D. degrees in electrical engineering from Tarbiat Modares University, Tehran, Iran, in 2008 and 2012, respectively. He received his first postdoc from the University of Beira Interior (UBI), Covilha, Portugal in 2015, while working on the 5.2-million-euro FP7 project SiNGULAR ("Smart and Sustainable Insular Electricity Grids Under Large-Scale Renewable Integration"). He received his second postdoc from the University of Salerno, Salerno, Italy in 2016. He is currently a Visiting Scientist (position only awarded to PhD holders who have scientific curricula of high merit, equivalent to Assistant Professor) and Senior Researcher at CMAST/UBI, where he has a major role of co-coordinating a WP in the 2.1-million-euro national project ESGRIDS ("Enhancing Smart GRIDS for Sustainability"), while co-supervising 5 PhD students and 2 post-doctoral fellows. He was considered one of the Outstanding Reviewers of IEEE TSTE, in 2014, and one of the IEEE TSG Best Reviewers in 2016. His research interests include power market simulation, market power monitoring, power system optimization, demand response, electric vehicles, price forecasting and smart grids.

João P. S. Catalão (M'04-SM'12) received the M.Sc. degree from the Instituto Superior Técnico (IST), Lisbon, Portugal, in 2003, and the Ph.D. degree and Habilitation for Full Professor ("Agregação") from the University of Beira Interior (UBI), Covilha, Portugal, in 2007 and 2013, respectively.

Currently, he is a Professor at the Faculty of Engineering of the University of Porto (FEUP), Porto, Portugal, and Researcher at INESC TEC, INESC-ID/IST-UL, and C-MAST/UBI. He was the Primary Coordinator of the EU-funded FP7 project SiNGULAR ("Smart and Sustainable Insular Electricity Grids Under Large-Scale Renewable Integration"), a 5.2-million-euro project involving 11 industry partners. He has authored or coauthored more than 500 publications, including 171 journal papers, 303 conference proceedings papers, 29 book chapters, and 14 technical reports, with an h-index of 30 and over 3735 citations (according to Google Scholar), having supervised more than 45 post-docs, Ph.D. and M.Sc. students. He is the Editor of the books entitled Electric Power Systems: Advanced Forecasting Techniques and Optimal Generation Scheduling and Smart and Sustainable Power Systems: Operations, Planning and Economics of Insular Electricity Grids (Boca Raton, FL, USA: CRC Press, 2012 and 2015, respectively). His research interests include power system operations and planning, hydro and thermal scheduling, wind and price forecasting, distributed renewable generation, demand response and smart grids. Prof. Catalão is an Editor of the IEEE Transactions on Smart Grid, an Editor of the IEEE Transactions on Sustainable Energy, an Editor of the IEEE Transactions on Power Systems, and an Associate Editor of the IET Renewable Power Generation. He was the Guest Editor-in-Chief for the Special Section on "Real-Time Demand Response" of the IEEE Transactions on Smart Grid, published in December 2012, and the Guest Editor-in-Chief for the Special Section on "Reserve and Flexibility for Handling Variability and Uncertainty of Renewable Generation" of the IEEE Transactions on Sustainable Energy, published in April 2016. He was the recipient of the 2011 Scientific Merit Award UBI-FE/Santander Universities and the 2012 Scientific Award UTL/Santander Totta. Also, he has won 4 Best Paper Awards at IEEE Conferences.